EE463 Static Power Conversion I
Term Project Final Report

Volt Motors

Mehmet Emre DOĞAN – 2374825
Gamze ÇELİK – 2304327
Ömer ŞEN – 2305415

Introduction

In this project, a DC Motor Drive will be designed and implemented. The drive will run a DC motor when it is supplied by an AC source. In this report, the steps of component selection will be given. Next, key points of design decisions will be provided. Then, computer simulations with motor models will be provided with the test results of the system from demo day and from previous tests that have been done so far will be shown. Finally, test results thermal calculations will be done and compared with actual results.

Component Selection

Table 1: Component and Price List

Component	Quantity	Price
IGBT - IXGH24N60C4D1	1	96
3 Phase FBR	1	120
1000 µF 400V Capacitor	1	200
LM2596	2	32.14
230:24 Transformer	1	252
Single Phase FBR	1	2.45
2200 µF Capacitor	2	140
TLP250	1	47.92
330Ω Resistor	2	0.88
ESP8266	1	75.94
ROE-0512	1	89.71
DSEI30-06A	1	33.08
Current Sensor - ACS712	1	47.26
Fuse	2	1.34
Heatsink	3	45
Fan	2	56
Voltmeter	3	162
Lamp	1	20
Banana Connector	6	49
Terminal Block	8	22.7
Box	2	150
Stripboard	2	25.83
Deep Socket	3	1.98

Switch	1	4.73
Total		1535,96

IGBT - IXGH24N60C4D1

One of the main components is IGBT used in the buck converter. IXGH24N60C4D1 has an appropriate rating for the application. Moreover, the main reason for choosing IXGH24N60C4D1 is that it is easy to access since there are many of them in the stock of the laboratory.

3 Phase FBR

The chosen model is compliant to the system with its ratings. However, the main reason to choose the rectifier is the type of its sockets. Its sockets are compatible with the cable terminals in the laboratory. It would be easier to replace it in case of failure.

1000 µF 400V Capacitor

In simulations, 1000uF provided decent enough ripple for the high voltage circuitry, when the rated current of the motor is drawn. Moreover, the 400V rating was chosen to be safe to the possible ringing may occur in the voltage.

LM2596

There is a need for creating 5VDC 12VDC low voltages for the MCU and cooling fans, respectively. Moreover, this stepping down operation needs to be in a regulated manner. The LM2596 has a built-in feedback mechanism, regulating the voltage to desired value. Furthermore, LM2596 Adjustable modules are cheap and easy to access. As a result, it is chosen.

230:24 Transformer

Using only one supply is a bonus to obtain that transformer is chosen. The ratio is chosen based on the required voltage at the secondary of the transformer.

Single Phase FBR

In order to convert stepped down AC voltage by transformer into dc voltage, a rectifier is required. Due to easy access and low-price compliant ratings, KBU2M is chosen.

2200 µF Capacitor

In simulations, 2x2200uF provided decent enough ripple for the low voltage adapter circuitry.

TLP250

To isolate the MCU and High voltage side, an Opto isolator is needed. Since this model was available in the lab, it was chosen.

330Ω Resistor

To limit the current and the voltage which goes into the LED side of an optocoupler, a resistance is required. According to the calculations 330-ohm was appropriate.

ESP8266

ESP8266 is used instead of an Arduino because it is cheaper, has wi-fi, has higher memory, has a higher core frequency, compatible with Arduino IDE, and lastly, it supports PWM at all pins. There are various MCUs available. However,

ROE-0512

For optocoupler isolated 12V is needed. To convert 5V to isolated 12V ROE-0512 was a perfect choice.

DSEI30-06A

DSEI-30-06A is a good option for our design with its price, ratings, and accessibility.

Current Sensor - ACS712

Initially current feedback is designed, and the system is designed according to it. However, during the implications, the sensor fails, yet it conducts the current that is supposed to. Therefore, it is not utilized but not removed.

Fuse

Different levels of fuses are used to protect our circuit against high currents and bugs due to the high currents.

Heatsink & Fan

Heatsinks and fans were used for cooling. Some components can reach high temperatures and at those temperatures, components do not operate properly. There is a video link to one of the tests showing the effect of the fan on the IGBT and the diode of the main buck converter.
https://youtu.be/r-FZcK4Lljk

Voltmeter

To read input voltages voltmeters were used. Used voltmeters have 20 - 500 V AC range.

Lamp

When the output is active the lamp is on to notify the user.

Banana Connector

For easy I/O connections banana connectors were used.

Terminal Block

To obtain a modular system, we prefer to use them. Also, it makes it easy to mount/unmount the subsystems.

Box

To provide safe and easy usage to the user, and also for aesthetic reasons.

Dip socket

It was placed because if TLP250 breaks it can be changed easily. Also, during the soldering process, TLP250 can also break due to high temperature so that dip socket was used.

Switch

Switch is used to power the ESP8266 since ESP8266 requires 5V to operate without booting bugs. To prevent these bugs a switch was used.

Design Decisions

As we discussed in the complete simulation report, we will use the topology consisting of a three-phase full bridge rectifier feeding a buck converter that eventually drives the motor. The main block diagram of the system is shown in Figure 1 and Figure 2. Moreover, to accomplish various bonuses, we have some other submodules.

The motor drive system is designed in a modular manner to make it easy to analyze and debug. As well as to avoid epic failures; for example, a total board failure due to the explosion caused by an arc born from not enough clearance in the AC mains line. Thanks to the modular approach, we were able to get rid of only the faulty parts and redesign only them, not the complete system.

Hence, the motor driver system consists of various subsystems, as the block diagrams suggest. Each subsystem will be handled in detail to guarantee the subsystems work properly not only standalone but also after the integration.

In Figure 3, the completely integrated and finished version of the system is shown.

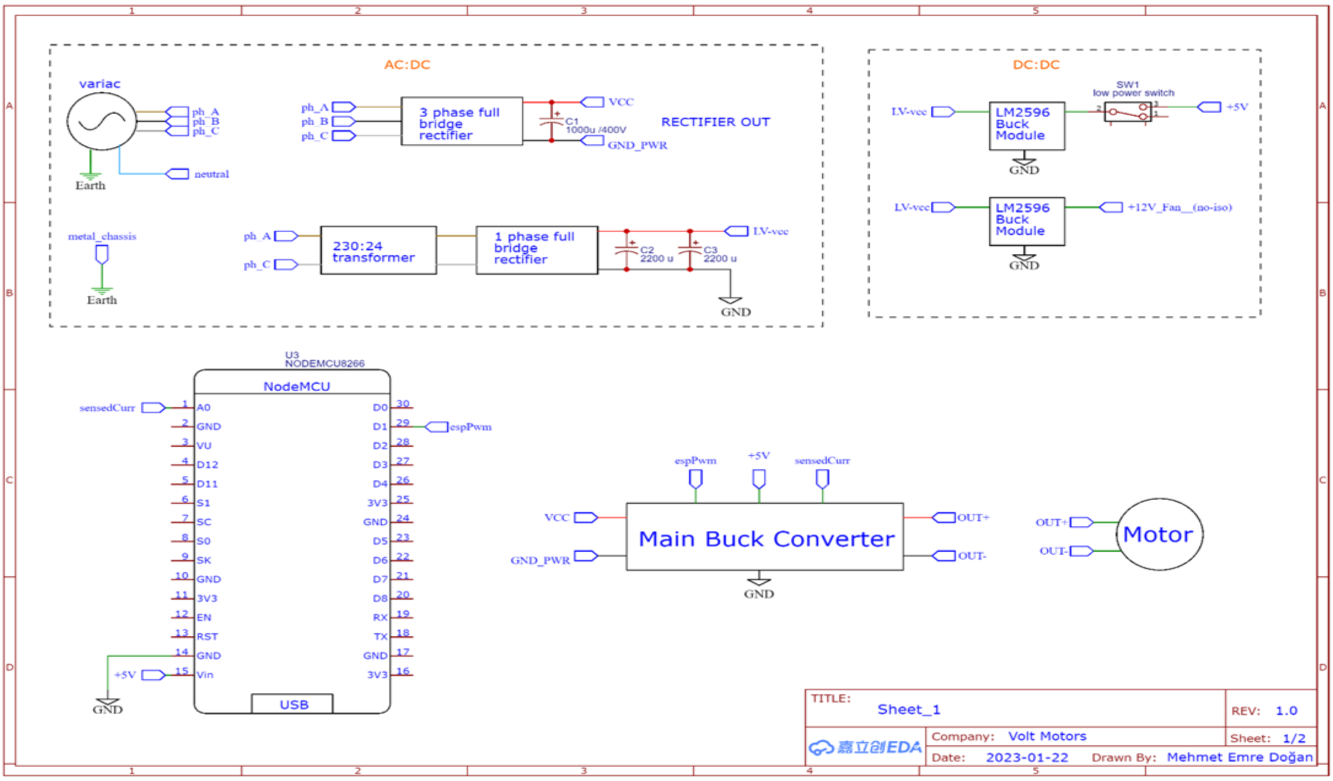

Figure 1: Main block diagram sheet 1

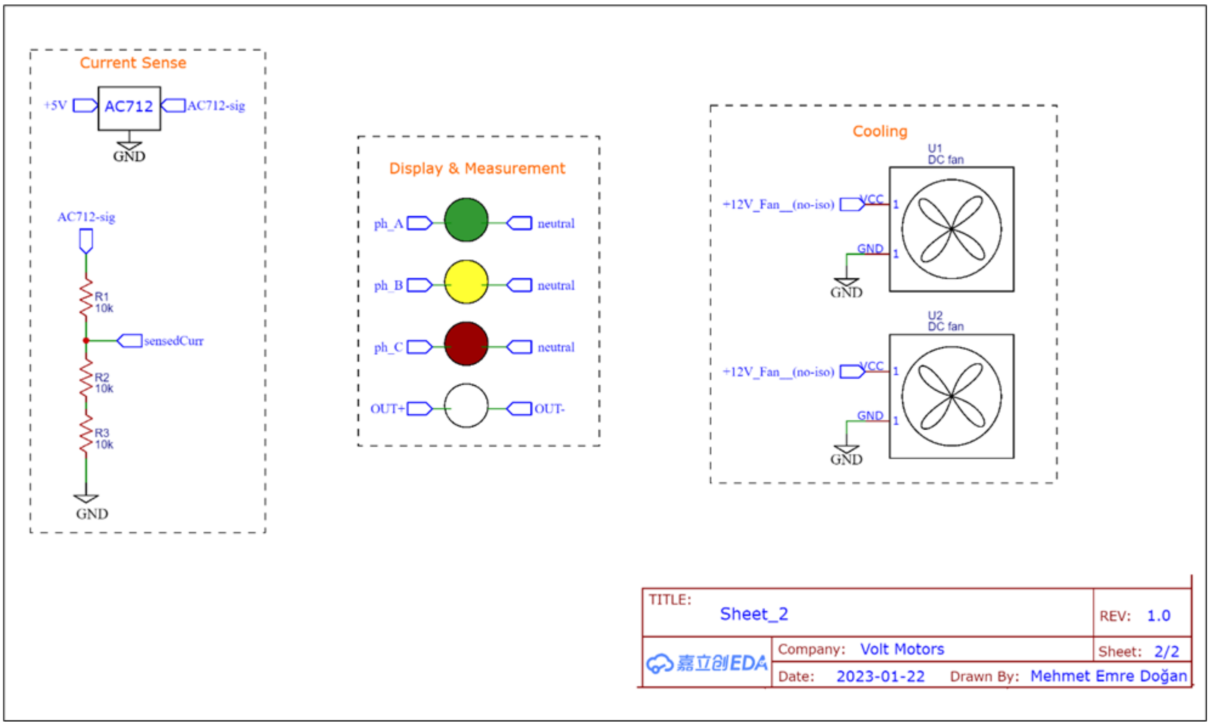

Figure 2: Main block diagram sheet 2

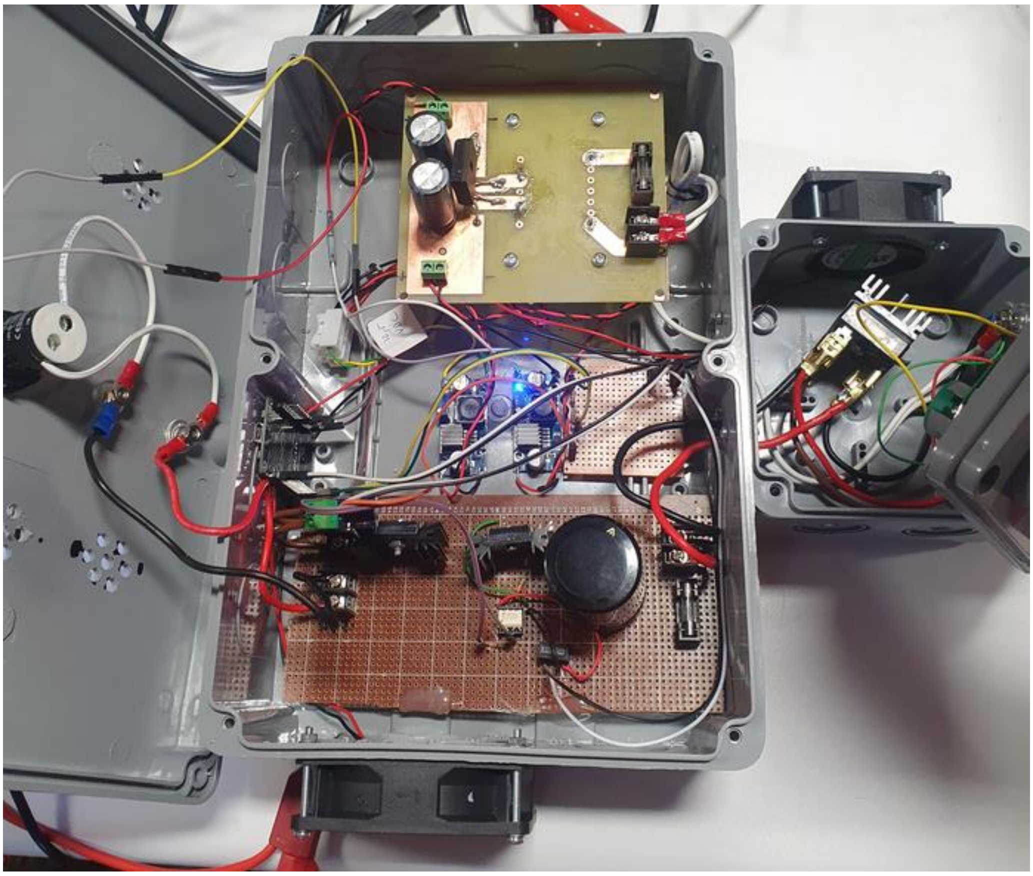

Figure 3: The completely integrated system from the demo day

AC-DC Converter Subsystem

To drive the DC motor, we need DC power. Moreover, to run the MCU (Micro-Controller-Unit) we also need low-power DC voltage, which needs to be isolated from the mains DC power.

3-Phase Full Bridge Rectifier + Capacitor

This rectifier, shown in Figure 4, rectifies the main AC power provided from the variac to DC 200V. Although the rated voltage of the motor is 180V DC, we rectify it to 200V DC because we plan to reach the rated voltage at 90% duty cycle. The discussion of why is provided in the Duty Cycle subsection of the MCU section. Then the voltage is smoothened (decreased its ripple) by the 1mF 400V polarized aluminum capacitor, shown in Figure 5, connected to the exit of the 3-Phase FBR.

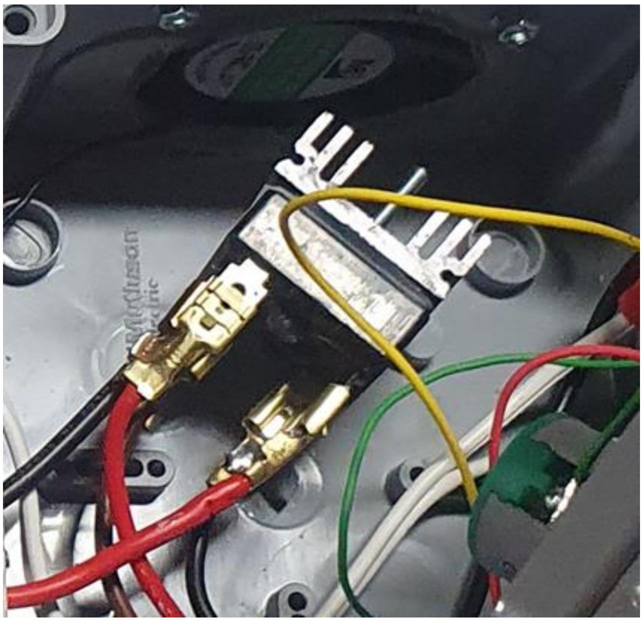

Figure 4: The 3-Phase FBR

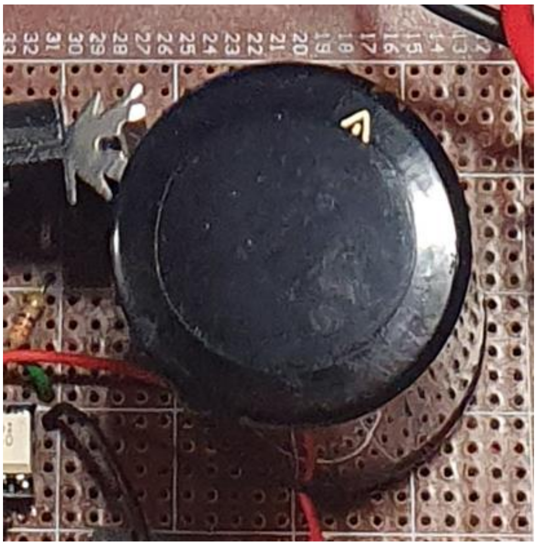

Figure 5: The Main Capacitor

Low Power Adapter

The low-power adapter schematic is shown in Figure 6. Its job is to provide low DC voltage to the LM2596 buck regulators to power MCU, fans, sensors, optoisolator, and other low-power devices.

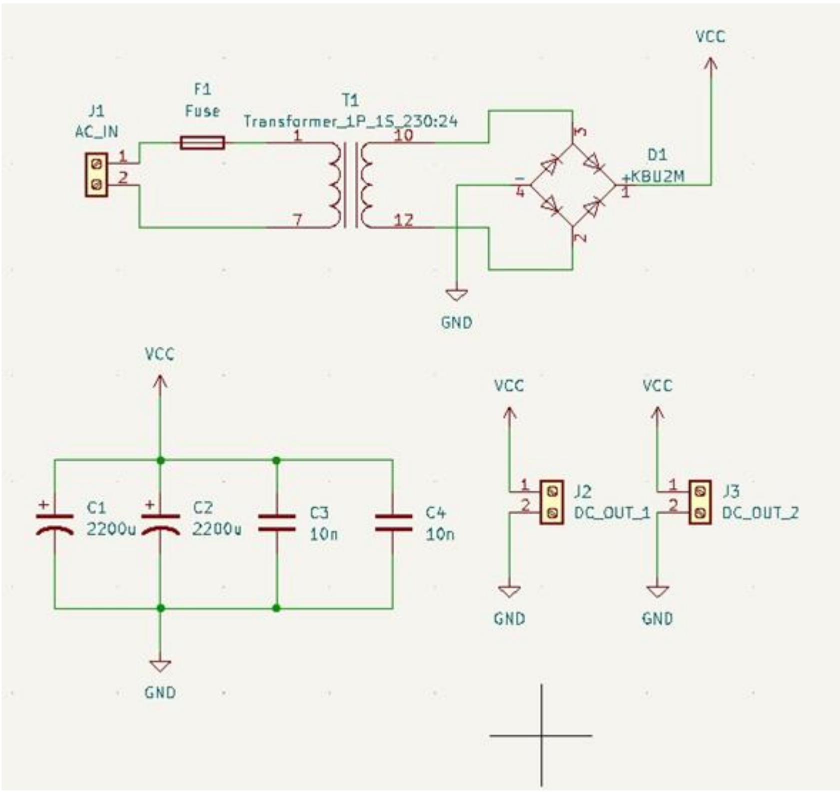

Figure 6: Low Power Adapter Schematic

This adapter, first, steps down the voltage using the transformer, then rectify with the single-phase FBR. Afterward, thanks to the large capacity of aluminum capacitors, the output ripple is smoothened. Moreover, in design, 2 ceramic capacitors are put to decrease the equivalent ESR of the subsystems of capacitors. However, these are not soldered in implementation since we did not have an ESR problem.

The fuse provides overcurrent protection and screwed terminal connectors ease making cable connections.

The VCC provided by this adapter is expected to be near 20VDC when two AC lines from the variac are connected to its AC_IN. Note that, the variac is adjusted to 85 V AC line to neutral, resulting in 148 V AC line to line.

However, since the transformer is nearly unloaded, due to the low-power devices connected, this output voltage is expected to increase. However, thanks to the 36 V DC maximum input voltage and built-in feedback and filter system of LM2596 buck regulator modules, neither this voltage rise nor the ripples are a problem. LM2596 modules provide clean and consistent voltages to MCU and other low-voltage peripherals.

The PCB design and an image from the demo day are shown for the adapter in Figure 7 and Figure 8, respectively.

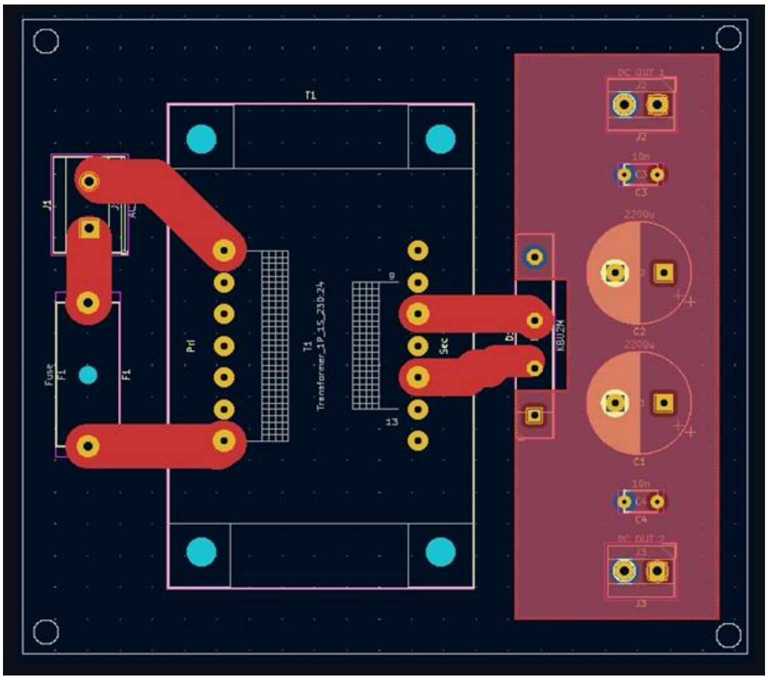

Figure 7: The low-power adapter PCB

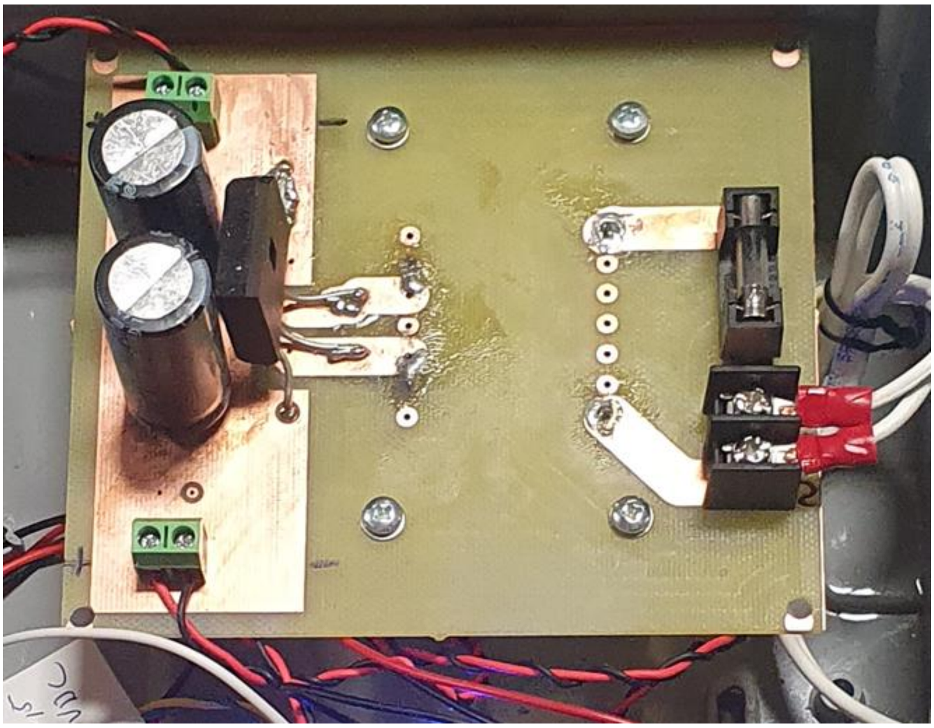

Figure 8: The low-power adapter from the demo day

Main Buck Converter Subsystem

The main buck converter's schematic is shown in Figure 9. The schematic includes 5 VDC and GND busbars to power the peripherals.

The output of the 3-Phase FBR is connected to the board using screw terminals. This voltage is filtered out via a 1 mF 400V aluminum capacitor, shown in Figure 5. The additional 10 nF ceramic capacitor is added to the design in case we had an ESR problem. But in implementation, it is not soldered since we had no ESR problems. Then this voltage passes a protective fuse and is called VCC, or VCC_PWR.

The isolated DC-DC converter creates an isolated +12VDC from the mains 5VDC to feed into the optocoupler's VCC and GND.

The optoisolator receives the PWM signal from the ESP and amplifies it in an isolated manner to drive the gate of the IGBT. 330 Ohm of resistors is connected in series to the LED part of the Opto to limit current. The Opto's forward voltage is near 1.8 Volts and this resistor guarantees the ESP provides current to the Opto less than 10 mA.

The resistor between the Opto’s output and the gate of the IGBT is also 330 Ohms because it works. We first tried 330 Ohm and it worked perfectly, then we did not change it.

The freewheeling diode parallel to the output of the converter makes sure the current due to the inductance of the motor can have a path to circulate when the IGBT is on OFF duty. Therefore, the IGBT is protected from damages due to overvoltage caused by the motor inductance.

The current sensor is connected via the screw terminals to measure the current drawn. The screw terminals ease the change of the sensor in case of failure.

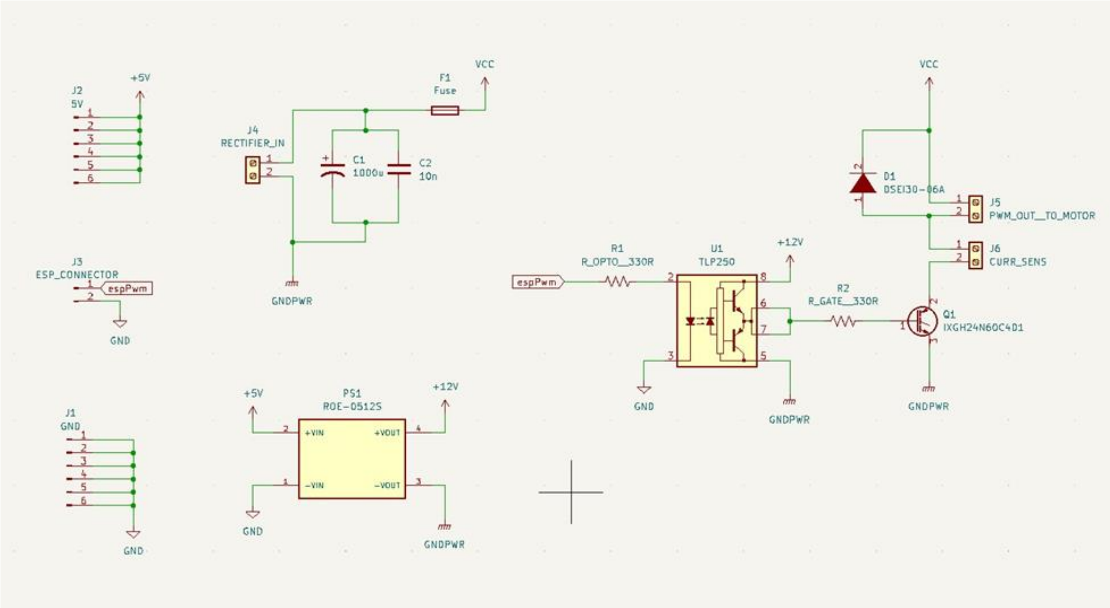

Figure 9: main Buck Converter

Figure 10: The failed main buck PCB

We designed a PCB for the Main Buck Converter, as shown in Figure 10. However, it failed due to some known and unknown reasons.

One of the known reasons is that the PCB has been wrongly produced. The positive pin of the Opto's LED is shorted to the ground because of a manufacturing error. The error is understood by comparing Figure 11 with Figure 10.

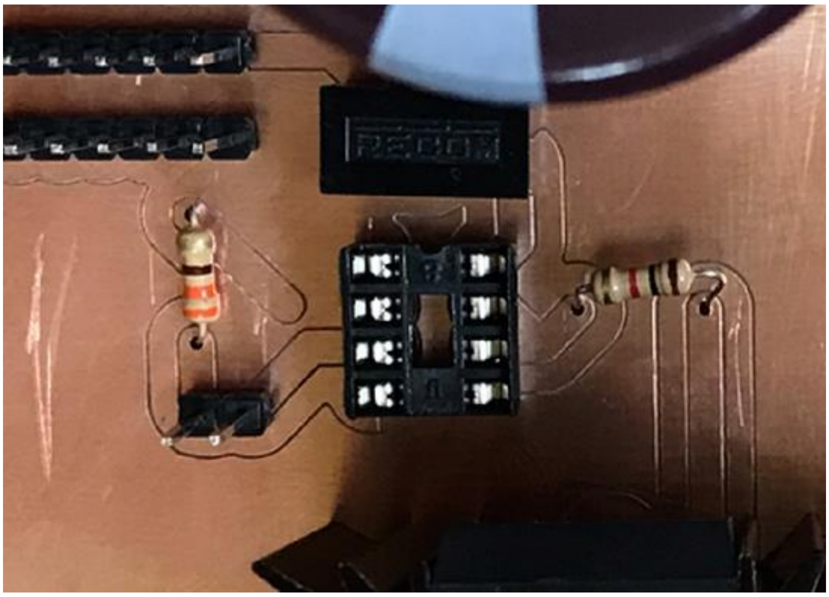

Figure 11: The Opto LED positive input, manufactured

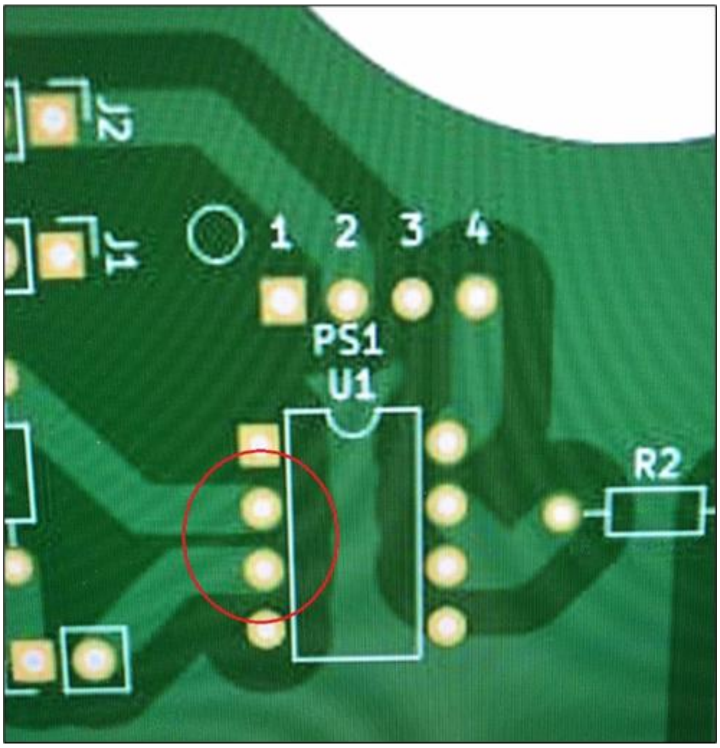

Figure 12: The Opto LED inputs, designed

Although we solved this problem by bending the optoisolator's LED pins and space soldered these pins. However, unfortunately, the board was still not working due to the errors we were unable to diagnose. Afterward, we rebuilt the buck circuit on the stripboard before the demo, as shown in Figure 13.

Thanks to the modularity approach, we were able to use the rest of the designs without any problems.

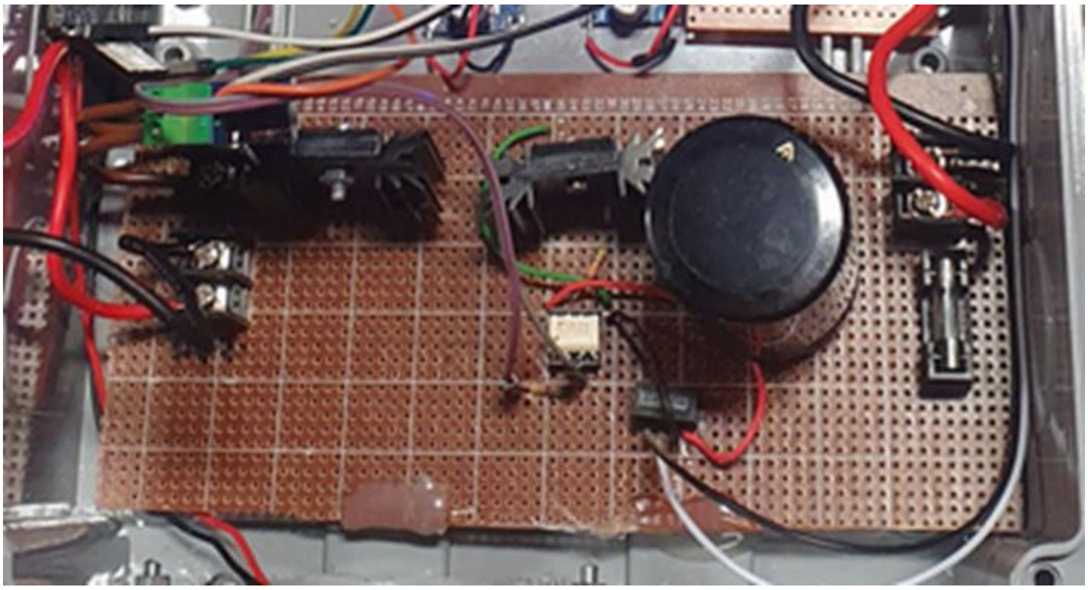

Figure 13: The buck converter on the stripboard

MCU & Software Subsystem

The MCU subsystem is responsible to generate the PWM signal with the duty cycle that the users select via the modern Web GUI (Graphical User Interface), as shown in Figure 14. Moreover, as shown in Figure 14, the software has a WebSerisal to print timestamped important run-time data.

The online Web GUI demo is available [1]. Note that the Set Direction and Close Loop menus are inactive due to the system not including H-Bridge and Close Loop Speed Sensor. However, these menus exist for future versions of our design updates.

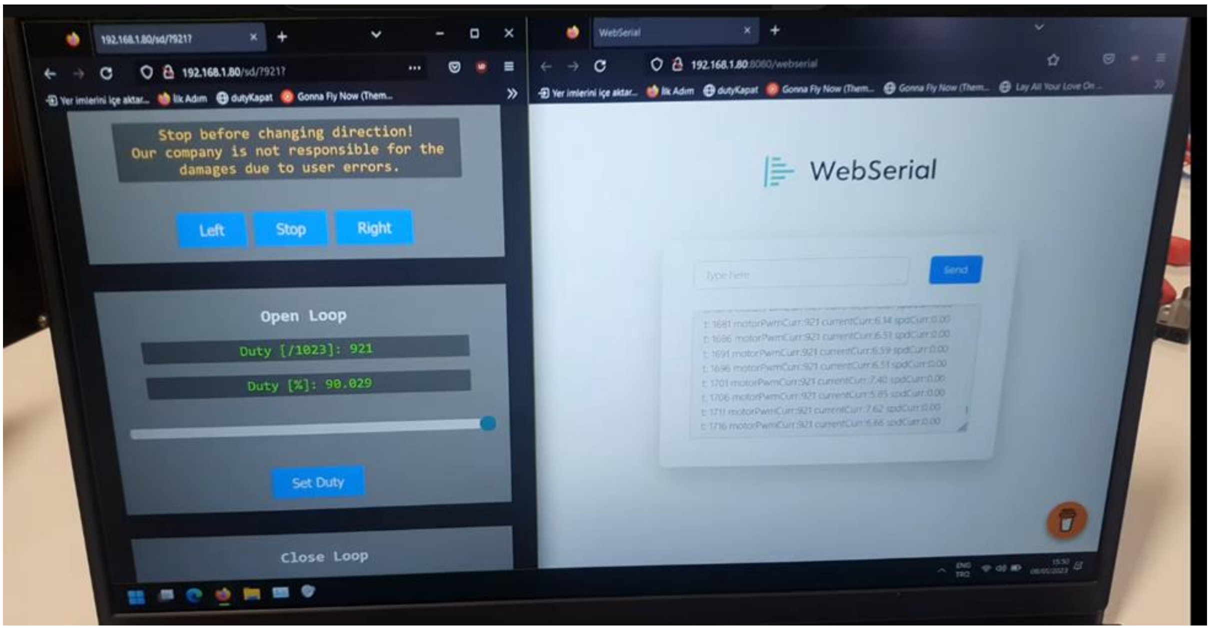

Figure 14: WebGui with WebSerial from demo day

Duty Cycle

The duty cycle is adjusted using the slide bar shown in Figure 15. The range of the used duty cycle is 0.1-0.9. That is, the motor reaches its rated speed and power with the duty cycle at 90%, instead of 100%. The reason for that approach is to avoid unstable switching at 0% (fully off) and 100% (fully on) by providing a safety margin. For example, due to environmental noise, the PWM signal may deviate slightly from the adjusted duty, and the safety margin makes sure this deviation will not change the state of the system.

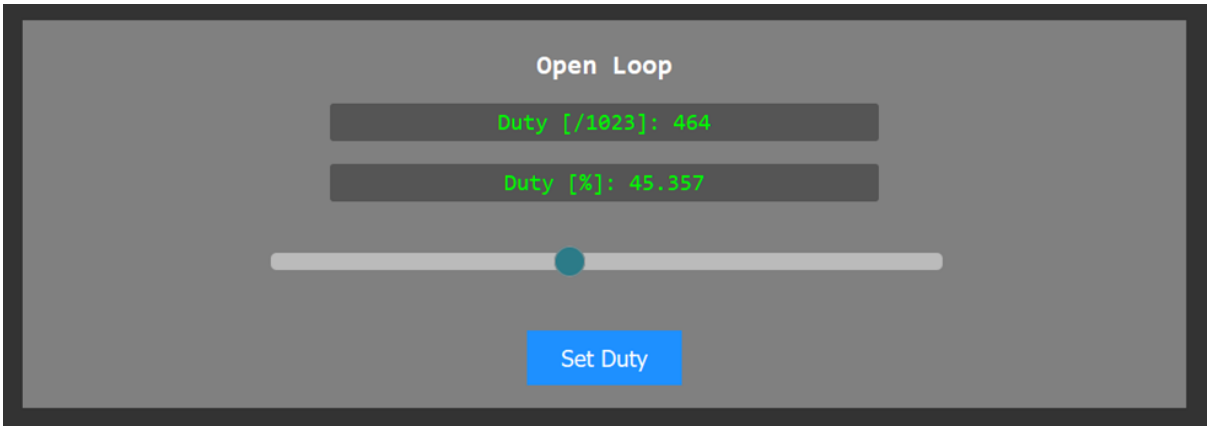

Figure 15: Open-loop duty selector slide-bar

Ramping Duty Cycle

The duty cycle is slowly increased and decreased to avoid the inrush currents in the motor starting as well as to decrease the effect of transient spikes that may be caused by fastly changing the duty cycle. This operation has a video demo [2], and a scene from this video is shown in Figure 16.

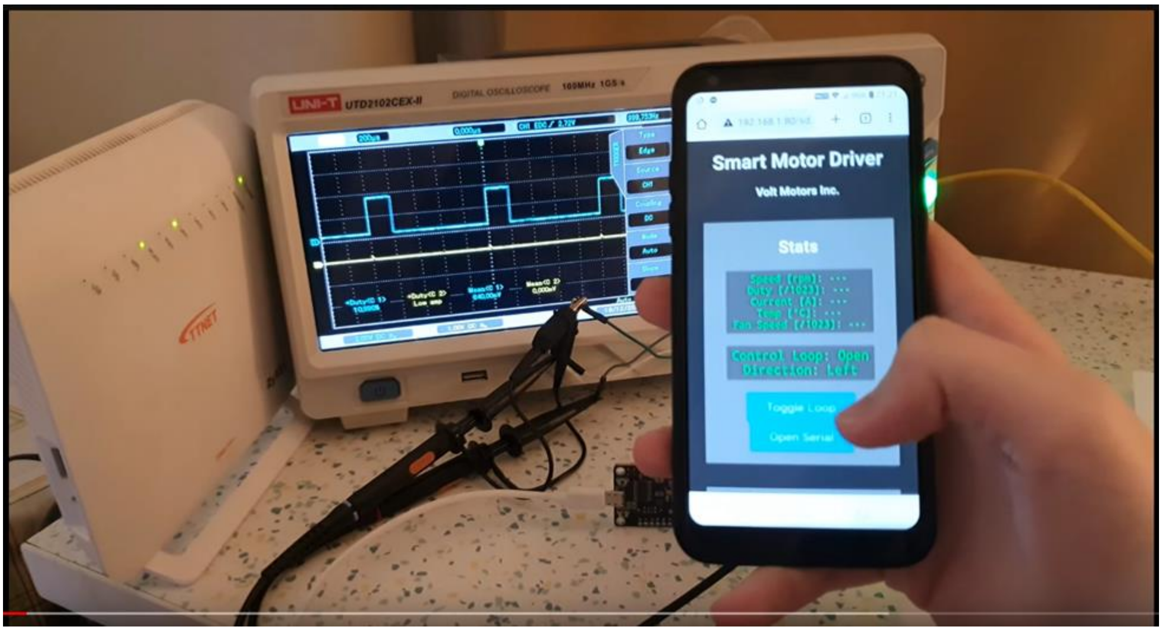

Figure 16: YouTube: ESP8266 Ramp PWM via Web GUI

Switching Frequency

The switching frequency of the generated PWM signal is chosen as 1 kHz since the Main Buck Converter uses an IGBT to switch the motor. We know that the IGBTs are not capable of switching at high frequencies due to their high-rise time and turn-on/off delay times, in addition to their huge switching energy. For example, we used IXGH24N60C4D1 N channel IGBT, whose switching energy is 1.46 mJ. On the other hand, LSIC1MO120E0080 N Channel SiC MOSFET only has 0.25 mJ of switching energy.

Moreover, designing a circuity capable of high switching frequency requires more attention and expertise. For example, the paths carrying the PWM signal should be properly engineered. However, due to our modular approach, we use jumper cables to carry the PWM signal.

As a result, on the first try, we used 1 kHz as the switching frequency. Afterward, we continued with that frequency because the integrated whole system worked pretty decent with a 1 kHz frequency.

Power

The used board NodeMcu ESP8266 needs +5VDC from its Vin pin. The required voltage is supplied by an LM2596 buck regulator. Moreover, a small switch is attached in series to avoid booting bugs caused by the slowly increasing variac voltage. Thanks to that switch, we power on the ESP manually when the variac voltage reaches its rated value.

Current Sensor

ACS712 Current sensor measures the motor current for debug purposes. Unfortunately, the existing ACS712 was burned due to misconnections, and replaced with another. However, since the current scale of the new one is different, the reading is wrong. The code needed to be updated but since it was the last day, we do not want to cause further bugs by editing the code, we did not edit.

In the future, a current feedback loop control could be added by just a software update thanks to the current sensor.

Voltage Divider

To convert the 5 V analog level of the current sensor to the 3.3 V analog level of the ESP, a resistor divider network is used.

Display & Measurement Subsystem

This subsystem consists of three voltmeters connected in a wye configuration to measure line-to-neutral input voltages. Moreover, a signal lamp is connected to the output to signal when the output is enabled.

Cooling Subsystem

This subsystem consists of two 12V DC fans. One for cooling the three-phase rectifier, one for the IGBT and diode of the Main Buck Converter.

Computer Simulations and Test Results

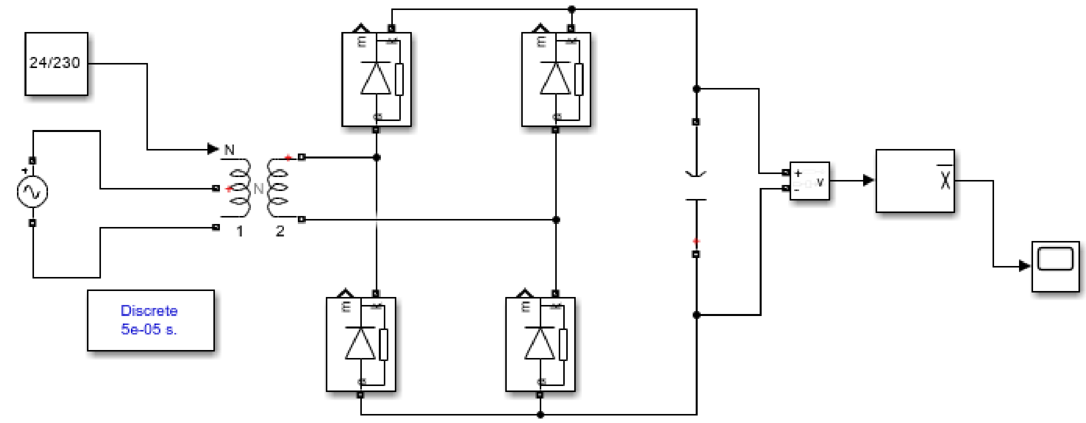

Figure 17: Transformer Simulation Schematic

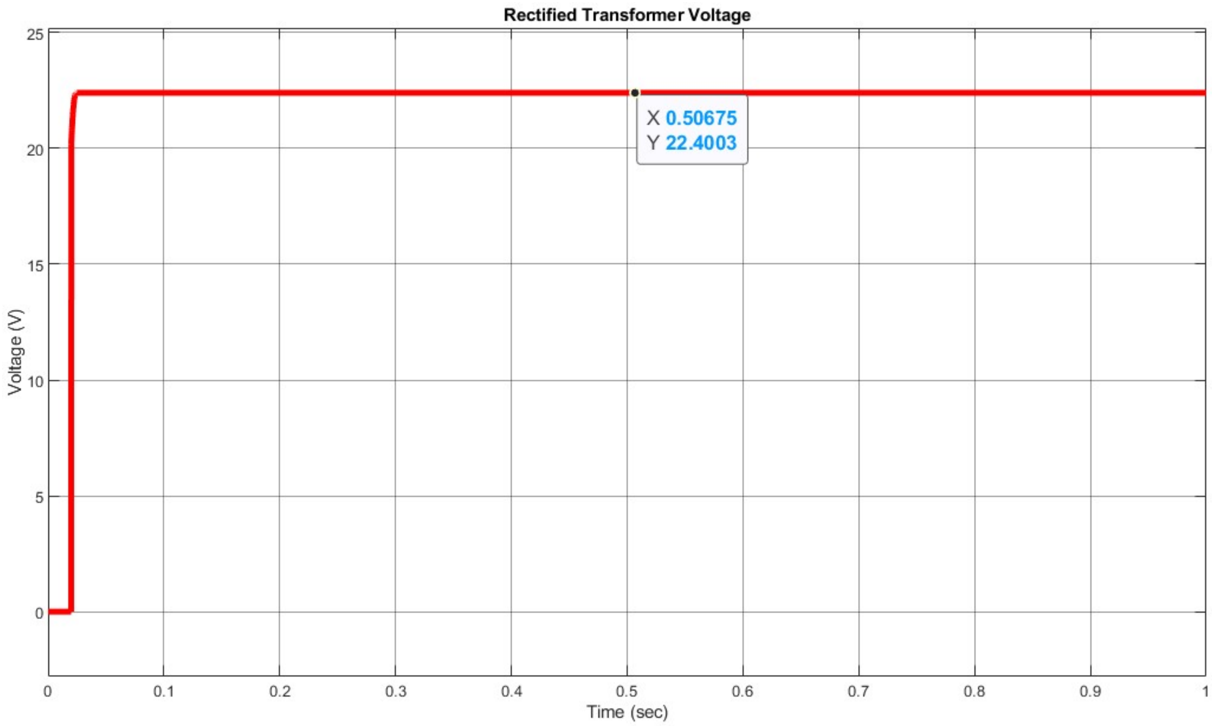

Figure 18: Transformer Simulation Results

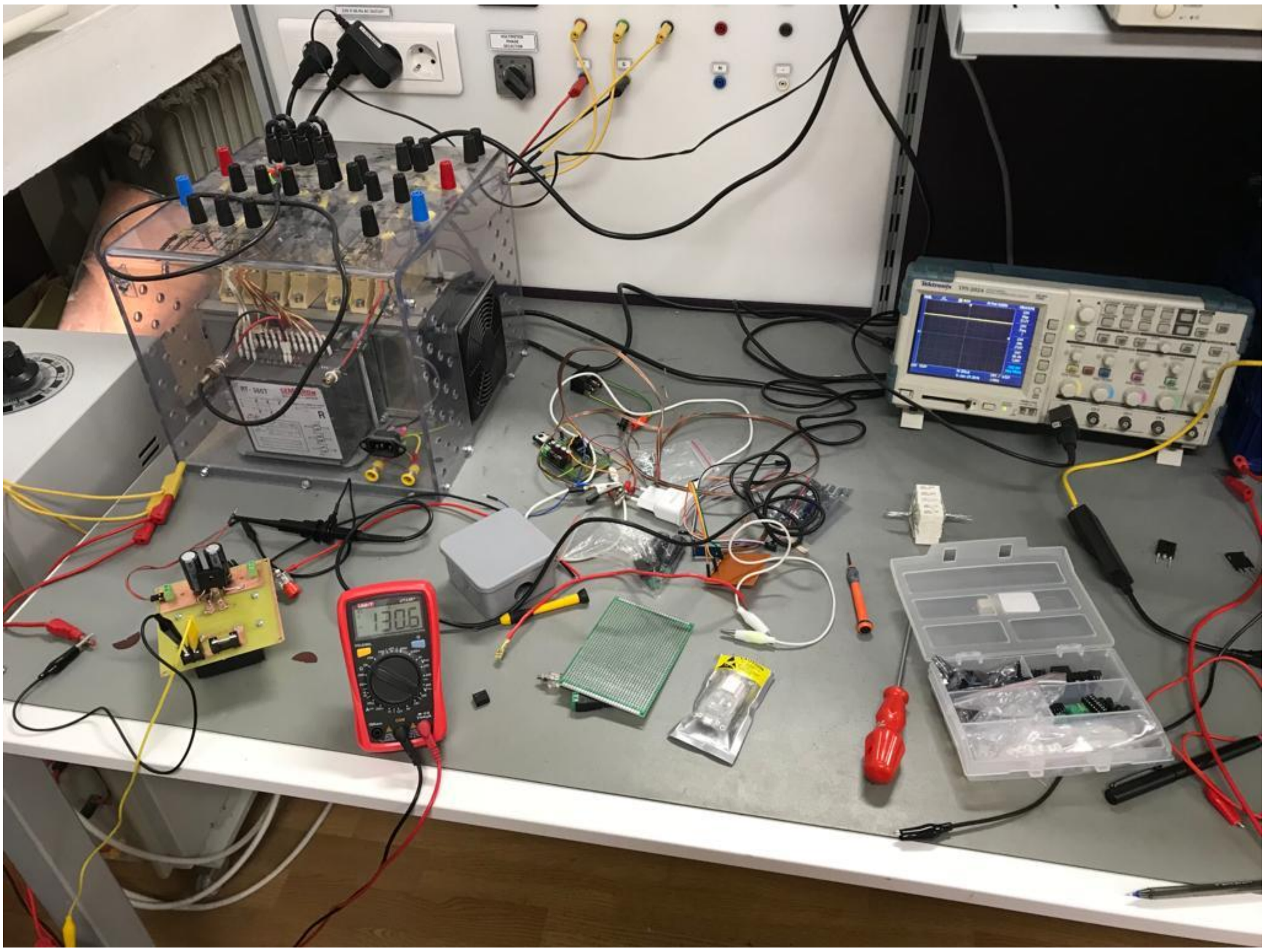

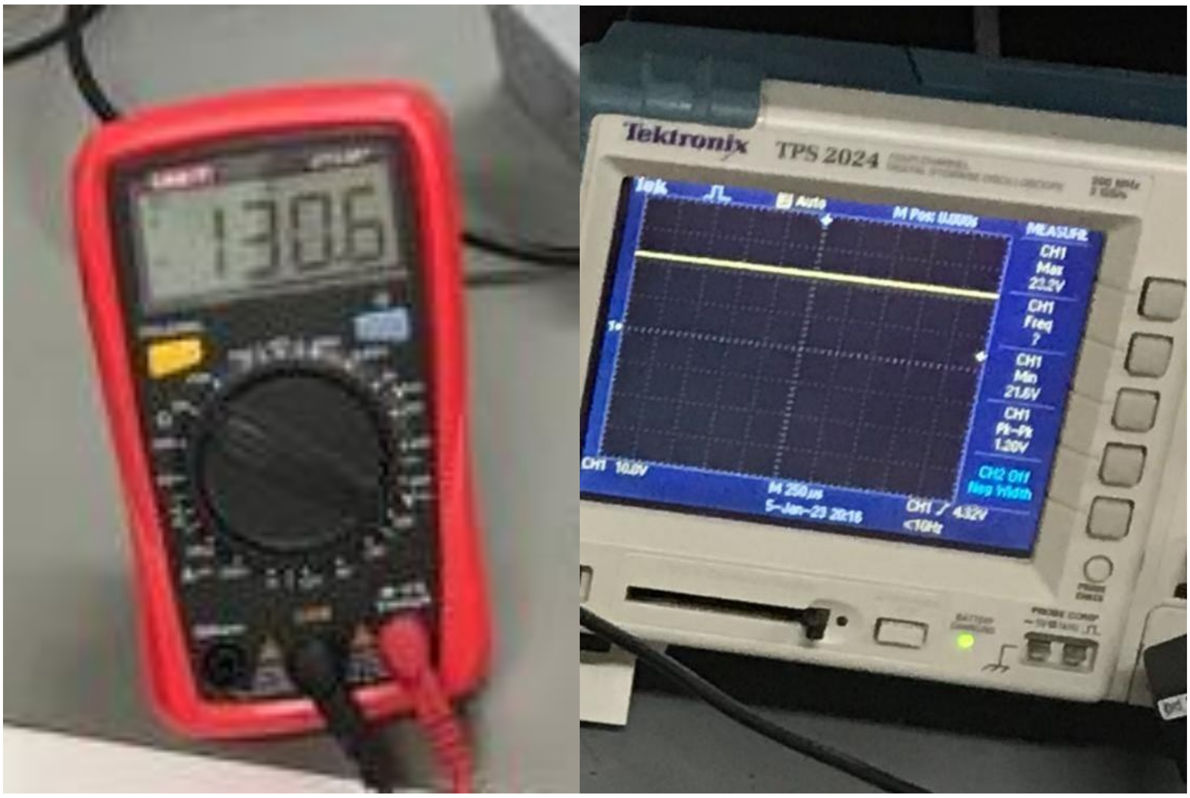

Figure 19: Transformer Test Result for V_{LL},rms=130V

In the simulations, it has been found that expected output voltage of the single supply transformer system is around 22.4 Volt DC. During the implementation, tests show that the implemented system provides approximately 22.4 Volt, which is almost the same. Output rectified voltage is provided to LM2596 Adjustable Voltage Step Down Power Module (4-35V Input - 1-30V Output) in order to provide power to lover voltage components, such as fans, controllers.

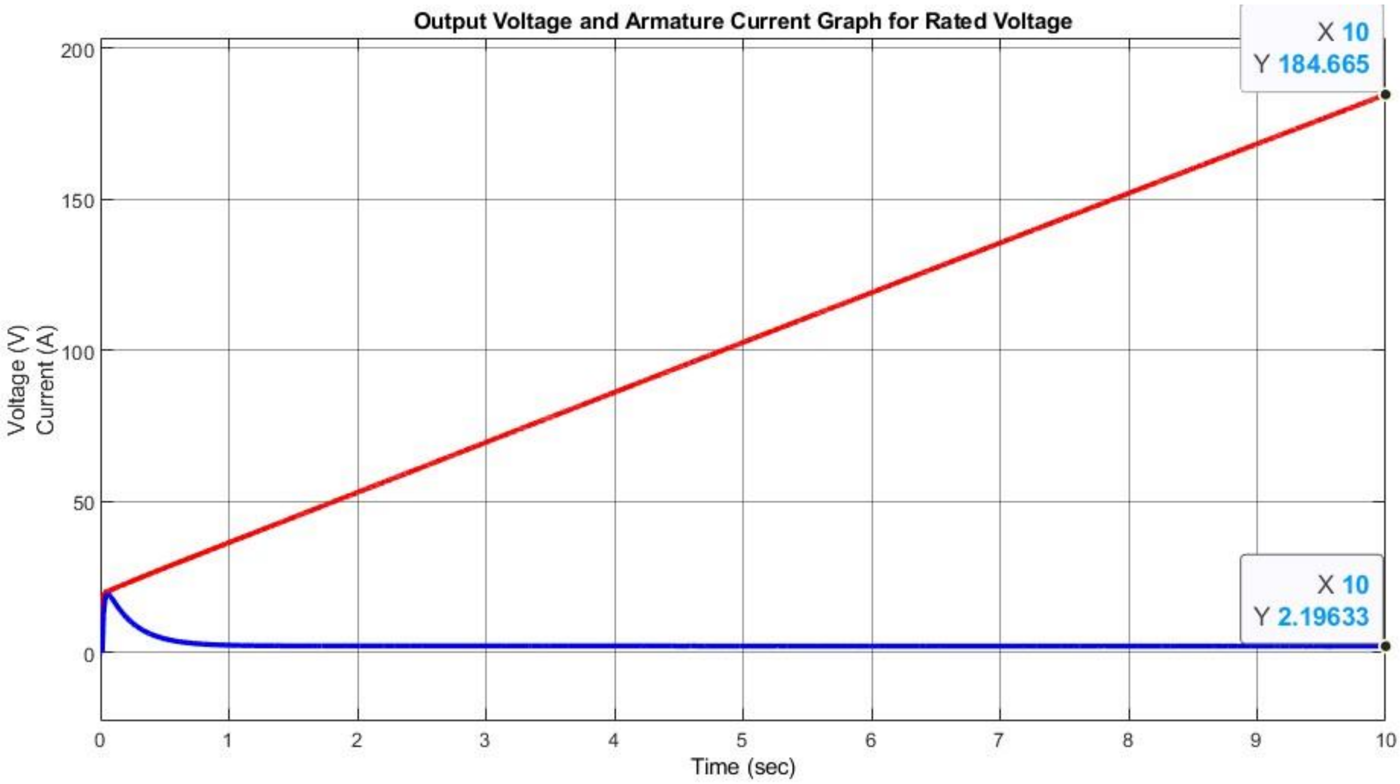

Figure 20: Output Voltage and Armature Current for Rated Voltage

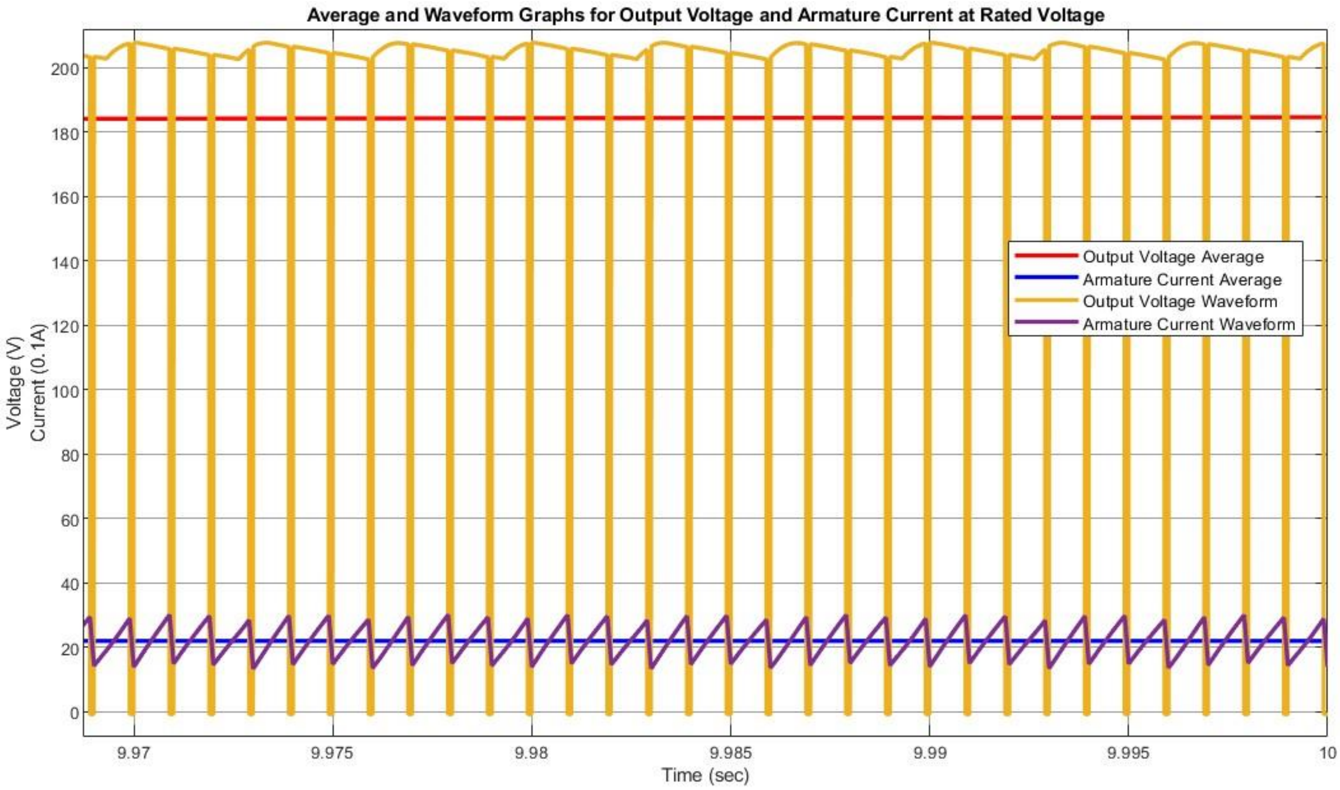

Figure 21: Average and Waveform Graphs for Output Voltage and Armature Current at Rated Voltage

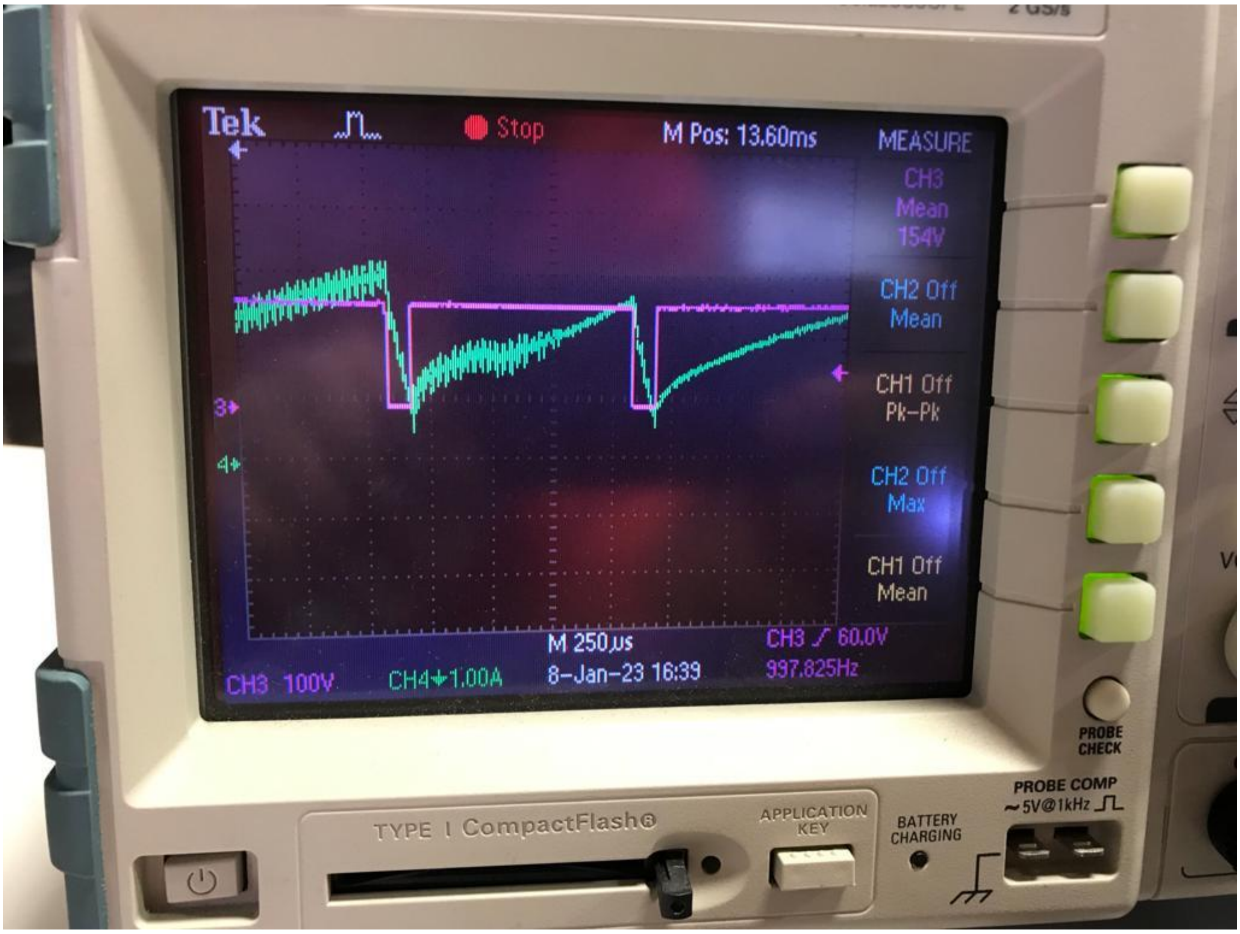

Figure 22: Armature Current Waveform

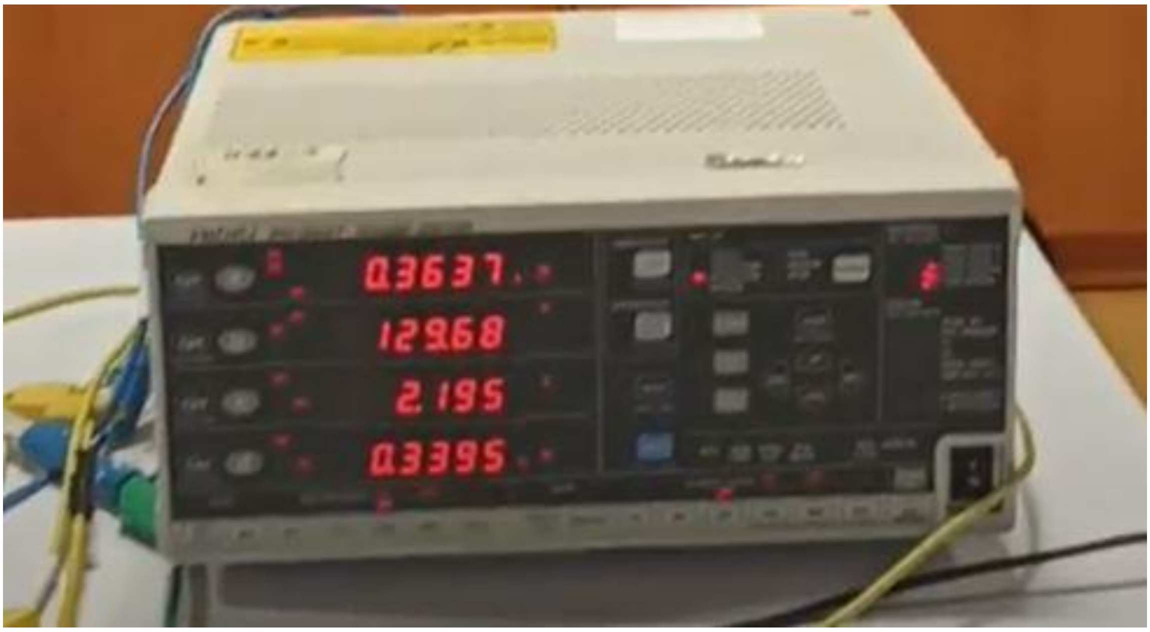

Figure 23: Voltage and Power Ratings for Rated Voltage

Previous 4 Figures, Figure 20 to 23, show the simulation and test results of rated voltage of the system without load. Figure 20 simulation results show the output voltage average as 184.6V and Figure 23 show the actual test results which show output line to line voltage as 130V. For 130V line to line input voltage, output voltage can be seen from Figure 22. Peak of the purple graph is around 200V and the duty cycle is 0.9. Therefore, output average voltage is around 180V, which is expected from the simulation result Figure 20. The Figure 21 shows the simulation results for the waveforms. Notice that the current waveform is scaled with 0.1A. As can be seen from the test results at Figure 22, test results and simulation results are compliant with each other. The efficiency is found as 0.340kW/0.364kW=94% during the tests.

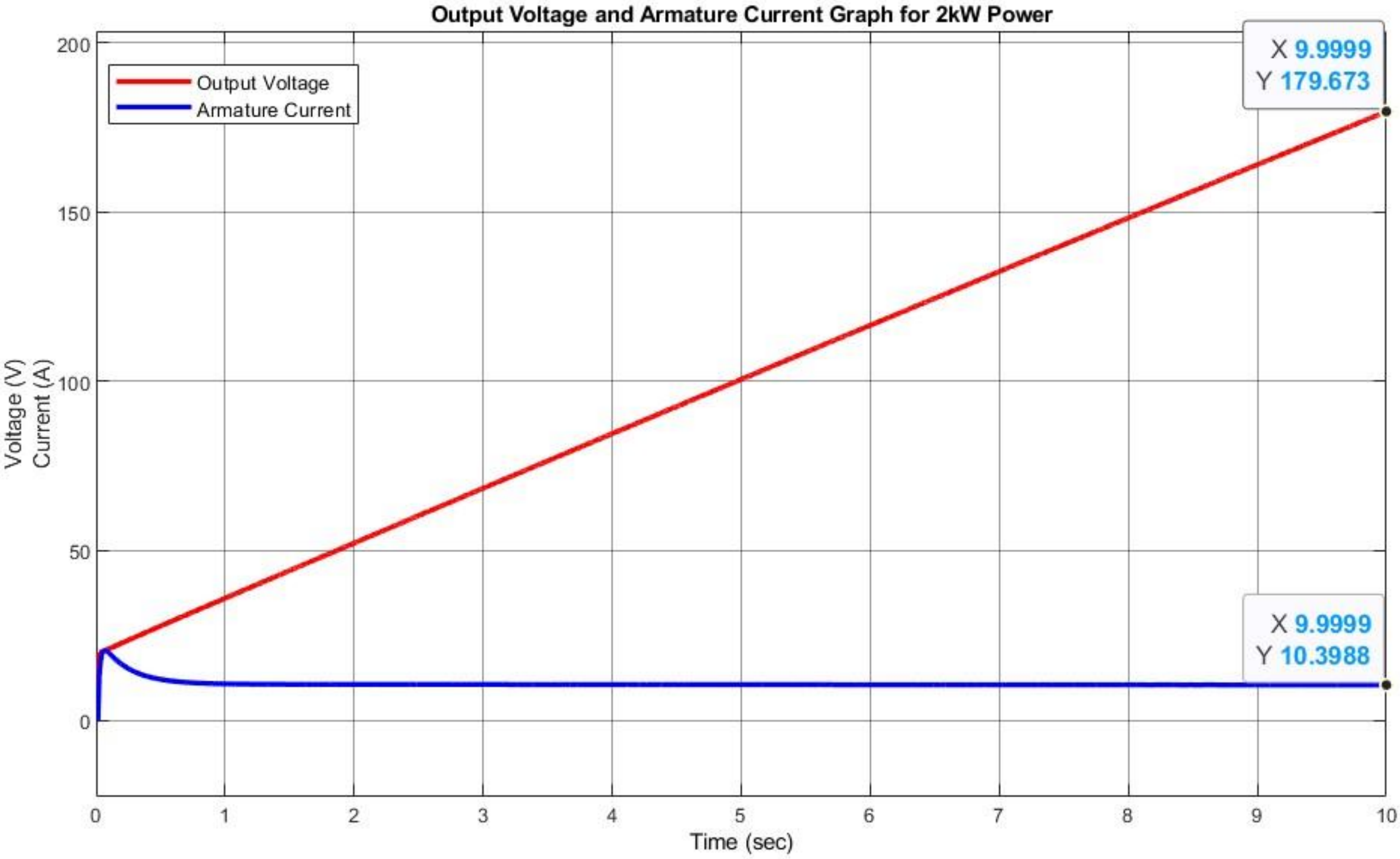

Figure 24: Output Voltage and Armature Current for 2kW Power

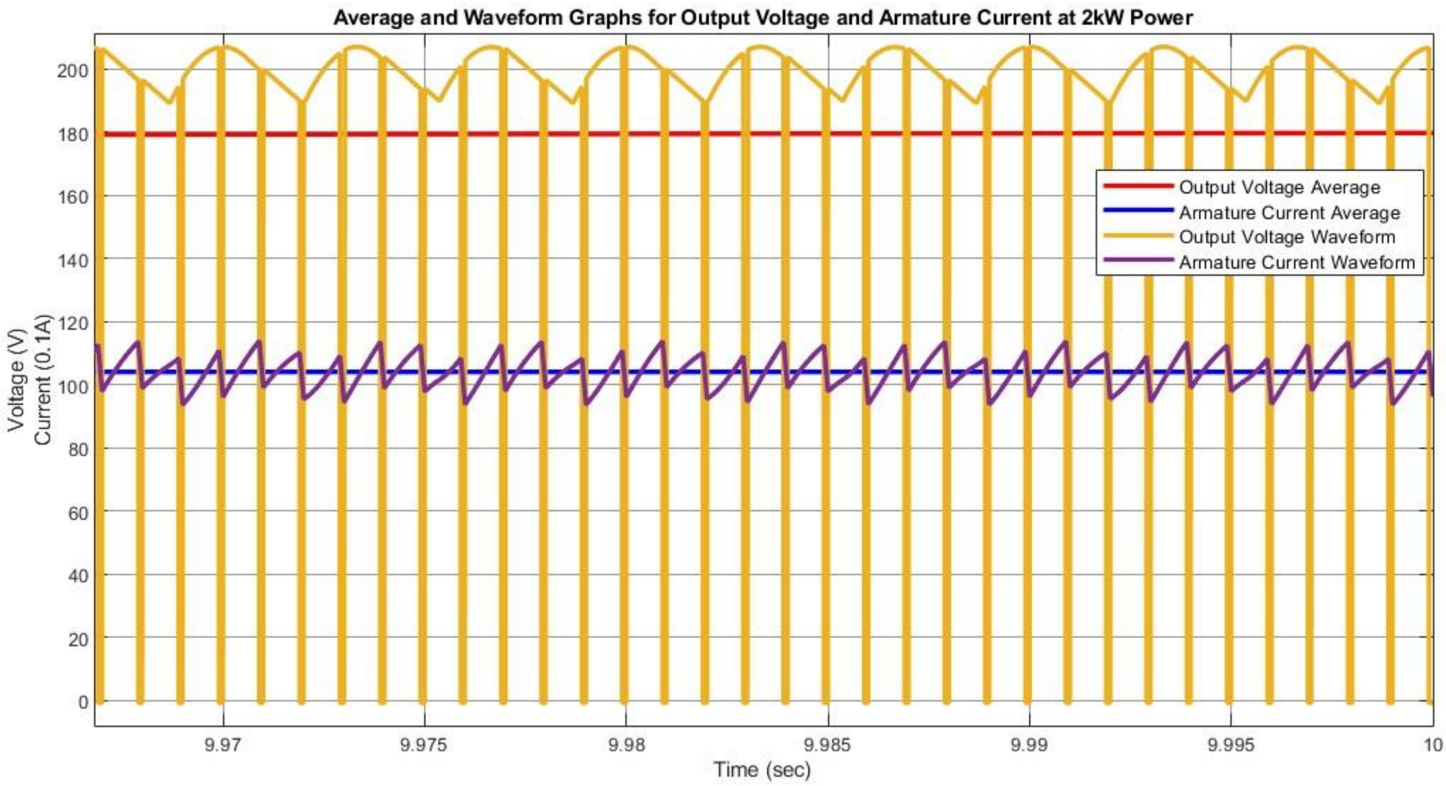

Figure 25: Average and Waveform Graphs for Output Voltage and Armature Current at 2kW

Figure 26: Armature Current Waveform

Figure 27: Voltage and Power Ratings for 2kW Power

Previous 4 Figures, Figure 24 to 27, show the simulation and test results of the system at 2kW Power input. Figure 24 simulation results show the output voltage around 180V and Figure 27 show the actual test results which show output line to line voltage as 160V. For 160V line to line input voltage, output voltage can be seen from Figure 26. Unfortunately, there is no clear view of the output voltage waveform. However, it is known that output voltage is around 180V. The test results are a bit different from the simulation results, which have input line to line voltage as 130V. The reason behind this difference is that when drawn current increases, the capacitance of the capacitor becomes insufficient, and ripples are increased. To provide the same output voltage and eliminate the negative effects of the ripples, input voltage is increased. Therefore, output average voltage is around 180V for a higher input voltage. The Figure 25 shows the simulation results for the waveforms. Notice that the current waveform is scaled with 0.1A. As can be seen from the test results at Figure 26, test results and simulation results are compliant with each other. The efficiency is found as 1.911kW/1.982W=96% during the tests.

Thermal Calculations

$$P_{loss,conduction,IGBT} = V_{CE,sat} \cdot I_{avg} \cdot Duty \cong 1.9V \cdot 10.4A \cdot 0.9 = 17.784W$$

$$P_{loss,switching,IGBT} = E_{switching,total} \cdot f_{switching} \cong 1.46mJ \cdot 1kHz = 1.46\ W$$

$$P_{loss,total,IGBT} = 19.244W$$

$$P_{loss,conduction,diode} = V_{fwd} \cdot I_{avg} \cdot (1 - Duty) \cong 1.52V \cdot 10.4A \cdot 0.1 = 1.58W$$

$$P_{loss,switching,diode} = (\frac{1}{2} \cdot C_R \cdot {V_R}^2 + \frac{1}{6} \cdot I_{RR} \cdot V_R \cdot t_b) \cdot f_{switching}$$

$$\cong (\frac{1}{2} \cdot 2pF \cdot 600V^2 + \frac{1}{6} \cdot 9A \cdot 600V \cdot 150ns/2) \cdot 1kHz = 0.068\ W$$

$$P_{loss,total,diode} = 1.648W$$

$$T_{junction} = T_{ambient} + P_{loss} * R_{th,eq}$$

$$T_{IGBT} = T_{ambient} + P_{loss} * (R_{th,JC} + R_{th,HA}) = 17°C + 19.24W * (3.5°C/W + 0.8°C/W)$$
$$= 99.3°C$$

$$T_{Diode} = T_{ambient} + P_{loss} * (R_{th,JC} + R_{th,CH} + R_{th,HA})$$
$$= 17°C + 1.648W * (0.8°C/W + 0.25°C/W + 3.5°C/W) = 24.5°C$$

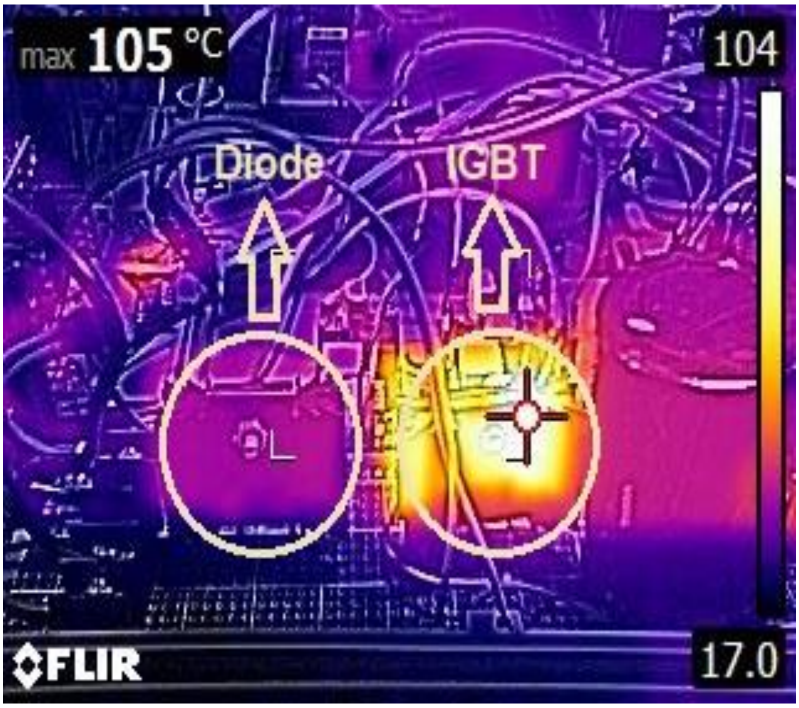

Figure 28: Thermal View of The Main Lossy Components

As can be seen from the Figure x, the IGBT reaches the temperature 105°C, which is calculated as 99.3°C in the calculations. The reason for the difference is that the thermal resistance between case to heatsink is not specified in the datasheet; therefore, missing components of the thermal resistance equivalent results as a minor difference between calculations and actual results. For the diode, calculated temperature is observed during the 2kW operation, which is expected.

Conclusion

In conclusion, the project aimed to design and implement a DC Motor Drive that could run a DC motor when supplied with an AC source. The report discussed the design decisions and bonus topologies used, such as the single supply bonus, PCB bonus, TEA bonus, and Box bonus, as well as providing computer simulations of the motor models. The process of component selection was also outlined, and test results from both demo day and previous tests were presented. These added bonuses have helped to increase the functionality and efficiency of the DC Motor Drive. Overall, the project was a success in achieving its goal of creating a functional and enhanced DC Motor Drive.

References

[1] M. E. Doğan, "ESP Webdemo," 2022. [Online]. Available: https://medogan.com/test_server_demo/463_esp_webdemo.html

[2] M. E. Doğan, "ESP8266 Ramp PWM via Web GUI," 2022. [Online]. Available: https://www.youtube.com/watch?v=6NDupYknA6s.

[3] G. Çelik, EE463 - Term Project Demo Video" 2023. [Online]. Available: https://youtu.be/3Q_IF74OBMI